

## CHAPTER 1

### The CFL phase and $m_s$ : An effective field theory approach

Thomas Schäfer

*Department of Physics  
North Carolina State University  
Raleigh, NC 27695*

We study the phase diagram of dense quark matter with an emphasis on the role of the strange quark mass. Our approach is based on two effective field theories (EFTs). The first is an EFT that describes quark quasi-particles near the Fermi surface. This EFT is valid at energies small compared to the chemical potential. The second is an EFT for the Goldstone modes in the paired phase. We find that in response to a non-zero strange quark mass the CFL phase first undergoes a transition to a kaon condensed phase, and then to a gapless phase with a non-zero Goldstone boson current.

#### 1. Introduction

Searching for exotic states of matter at high baryon density and high temperature is one of the central efforts in nuclear and particle physics. Calculations based on weak-coupling QCD indicate that the ground state of three flavor baryonic matter at very high density is the color-flavor-locked (CFL) phase<sup>1,2,3</sup>. The CFL phase is characterized by a pair condensate

$$\langle \psi_i^a C \gamma_5 \psi_j^b \rangle = (\delta_i^a \delta_j^b - \delta_j^a \delta_i^b) \phi. \quad (1)$$

This condensate leads to a gap in the excitation spectrum of all fermions and completely screens the gluonic interaction. Both the chiral  $SU(3)_L \times SU(3)_R$  and color  $SU(3)$  symmetry are broken, but a vector-like  $SU(3)$  flavor symmetry remains unbroken.

At baryon densities relevant to compact stars distortions of the ideal CFL state due to quark masses cannot be neglected<sup>4,5</sup>. The most important effect of a non-zero strange quark mass is that the light and strange quark Fermi momenta will no longer be equal. When the mismatch is much smaller than the gap one finds for degenerate quarks, we expect that it has little consequence, since at this level the original particle and hole states near the Fermi surface are mixed up anyway. On the other hand, when the mismatch is much larger than the gap, we expect that the ordering one finds in the symmetric system is disrupted, and that to a first approximation one can treat the light and heavy quark dynamics separately.

This argument is qualitatively right, but the correct picture turns out to be much more complicated, and much more interesting. The phase diagram of cold dense strange quark matter contains phases with kaon and eta condensates, phases with non-zero currents, and crystalline states. Performing systematic calculations of the properties of these states is not straightforward, even if the coupling is weak. A standard set of tools are Dyson-Schwinger equations. This approach becomes quite involved once the strange quark mass is taken into account, because there are many more gap parameters, and maintaining electric neutrality and color gauge invariance is difficult<sup>6,7,8</sup>. However, since chiral symmetry is broken in the CFL phase we know that the dependence on the quark masses is constrained by chiral symmetry. It is therefore natural to study the problem using effective field theories. In practice we will employ a two-step procedure. In the first step we match the microscopic theory, QCD, to an effective field theory of quasi-particles and holes in the vicinity of the Fermi surface. In the second step we match this theory to an effective chiral theory for the CFL phase.

## 2. High density effective theory

### 2.1. Effective field theory near the Fermi surface

The QCD Lagrangian in the presence of a chemical potential is given by

$$\mathcal{L} = \bar{\psi} (i\not{D} + \mu\gamma_0 - M) \psi - \frac{1}{4} G_{\mu\nu}^a G_{\mu\nu}^a, \quad (2)$$

where  $D_\mu = \partial_\mu + igA_\mu$  is the covariant derivative,  $M$  is the mass matrix and  $\mu$  is the baryon chemical potential. If the baryon density is very large perturbative QCD calculations can be simplified. The main observation is that the relevant degrees of freedom are particle and hole excitations in the vicinity of the Fermi surface. We shall describe these excitations in terms of the field  $\psi_v(x)$ , where  $v$  is the Fermi velocity. At tree level, the quark field  $\psi$  can be decomposed as  $\psi = \psi_{v,+} + \psi_{v,-}$  where  $\psi_{v,\pm} = P_{v,\pm}\psi$  with  $P_{v,\pm} = \frac{1}{2}(1 \pm \vec{\alpha} \cdot \hat{v})$ . Note that  $P_{v,\pm}$  is a projector on states with positive/negative energy. To leading order in  $1/\mu$  we can eliminate the field  $\psi_-$  using its equation of motion. The lagrangian for the  $\psi_+$  field is given by<sup>9,10,11</sup>

$$\mathcal{L} = \psi_v^\dagger \left( iv \cdot D - \frac{D_\perp^2}{2\mu} - \frac{g\sigma_{\mu\nu}G_\perp^{\mu\nu}}{4\mu} \right) \psi_v - \frac{1}{4} G_{\mu\nu}^a G_{\mu\nu}^a + \dots \quad (3)$$

with  $v_\mu = (1, \vec{v})$ . Note that  $v$  labels patches on the Fermi surface, and that the number of these patches grows as  $\mu^2$ . The leading order  $v \cdot D$  interaction does not connect quarks with different  $v$ , but soft gluons can be exchanged between quarks in different patches. In addition to that, there are four, six, ... fermion operators that contain fermion fields with different velocity labels. These operators are constrained by the condition that the sum of the velocities has to be zero.

In the case of four-fermion operators there are two kinds of interactions that satisfy this constraint, see Fig. 1. The first possibility is that both the incoming

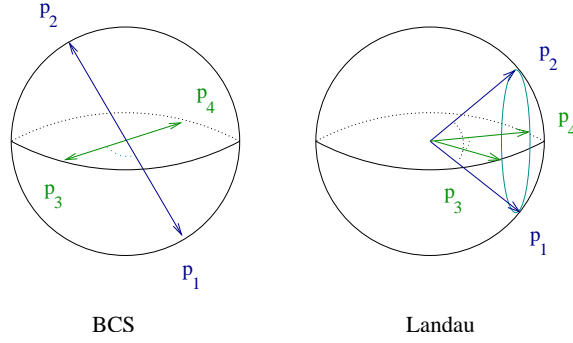


Fig. 1. Kinematics of four-fermion operators in the effective theory.

and outgoing fermion momenta are back-to-back. This corresponds to the BCS interaction

$$\mathcal{L} = \frac{1}{\mu^2} \sum_{v', \Gamma, \Gamma'} V_l^{\Gamma\Gamma'} R_l^{\Gamma\Gamma'}(\vec{v} \cdot \vec{v}') (\psi_v \Gamma \psi_{-v}) (\psi_{v'}^\dagger \Gamma' \psi_{-v'}^\dagger), \quad (4)$$

where  $\vec{v} \cdot \vec{v}' = \cos \theta$  is the scattering angle,  $R_l^{\Gamma\Gamma'}(x)$  is a set of orthogonal polynomials, and  $\Gamma, \Gamma'$  determine the color, flavor and spin structure. The second possibility is that the final momenta are equal to the initial momenta up to a rotation around the axis defined by the sum of the incoming momenta. The relevant four-fermion operator is

$$\mathcal{L} = \frac{1}{\mu^2} \sum_{v', \Gamma, \Gamma'} F_l^{\Gamma\Gamma'} R_l^{\Gamma\Gamma'}(\vec{v} \cdot \vec{v}') (\psi_v \Gamma \psi_{v'}) (\psi_{v'}^\dagger \Gamma' \psi_{v'}^\dagger). \quad (5)$$

In a system with short range interactions only the quantities  $F_l(0)$  are known as Fermi liquid parameters.

The effective field theory expansion is complicated by the fact that the number of patches  $N_v \sim \mu^2/\Lambda^2$  grows with the ratio of chemical potential  $\mu$  over the EFT cutoff  $\Lambda$ . This implies that some higher order contributions that are suppressed by  $1/\mu^2$  can be enhanced by powers of  $N_v$ . The natural solution to this problem is to sum the leading order diagrams in the large  $N_v$  limit<sup>12</sup>. In the gluon sector this corresponds to summing particle-hole loops in gluon  $n$ -point functions. There is a simple generating functional for these loop integrals which is known as the hard dense loop (HDL) effective action<sup>13</sup>

$$\mathcal{L}_{HDL} = -\frac{m^2}{2} \sum_v G_{\mu\alpha}^a \frac{v^\alpha v^\beta}{(v \cdot D)^2} G_{\mu\beta}^b. \quad (6)$$

In perturbation theory the dynamical gluon mass is given by  $m^2 = N_f g^2 \mu^2 / (4\pi^2)$ . In the fermion sector we have to consider four-fermion operators at leading order. Operators with six or more fermion fields are suppressed. The effective lagrangian

is given by

$$\begin{aligned} \mathcal{L} = & \psi_v^\dagger \left( i v \cdot D - \frac{D_\perp^2}{2\mu} \right) \psi_v - \frac{1}{4} G_{\mu\nu}^a G_{\mu\nu}^a + \mathcal{L}_{HDL} \\ & + \frac{1}{\mu^2} \sum_{v', \Gamma} \left[ F_l^\Gamma R_l^\Gamma(x) (\psi_v \Gamma \psi_{v'}) (\psi_v^\dagger \Gamma \psi_{v'}^\dagger) + V_l^\Gamma R_l^\Gamma(x) (\psi_v \Gamma \psi_{-v}) (\psi_{v'}^\dagger \Gamma \psi_{-v'}^\dagger) \right] + \dots \end{aligned} \quad (7)$$

## 2.2. Non-Fermi liquid effects

In this Section we briefly study the effective field theory in the regime  $\omega < m$  where  $\omega$  is the excitation energy and  $m$  is the effective gluon mass<sup>14</sup>. Since electric fields are screened the interaction at low energies is dominated by the exchange of magnetic gluons. The transverse gauge boson propagator is

$$D_{ij}(k) = \frac{i(\delta_{ij} - \hat{k}_i \hat{k}_j)}{k_0^2 - \vec{k}^2 + i\frac{\pi}{2} m^2 \frac{k_0}{\vec{k}}}, \quad (8)$$

where we have assumed that  $|k_0| < |\vec{k}|$ . We observe that the propagator becomes large in the regime  $|k_0| \sim |\vec{k}|^3/m^2$ . If the energy is small,  $|k_0| \ll m$ , then the typical energy is much smaller than the typical momentum,

$$|\vec{k}| \sim (m^2 |k_0|)^{1/3} \gg |k_0|. \quad (9)$$

This implies that the gluon is very far off its energy shell and not a propagating state. We can compute loop diagrams containing quarks and transverse gluons by picking up the pole in the quark propagator, and then integrating over the cut in the gluon propagator using the kinematics dictated by equ. (9). In order for a quark to absorb the large momentum carried by the gluons and stay close to the Fermi surface this momentum has to be transverse to the momentum of the quark. This means that the term  $k_\perp^2/(2\mu)$  in the quark propagator is relevant and has to be kept at leading order. Equation (9) shows that  $k_\perp^2/(2\mu) \gg k_0$  as  $k_0 \rightarrow 0$ . This means that the pole of the quark propagator is governed by the condition  $k_{||} \sim k_\perp^2/(2\mu)$ . We find

$$k_\perp \sim g^{2/3} \mu^{2/3} k_0^{1/3}, \quad k_{||} \sim g^{4/3} \mu^{1/3} k_0^{2/3}. \quad (10)$$

In the low energy regime propagators and vertices can be simplified even further. The quark and gluon propagators are

$$S_{\alpha\beta}(p) = \frac{i\delta_{\alpha\beta}}{p_0 - p_{||} - \frac{p_\perp^2}{2\mu} + i\epsilon \text{sgn}(p_0)}, \quad (11)$$

$$D_{ij}(k) = \frac{-i\delta_{ij}}{k_\perp^2 - i\frac{\pi}{2} m^2 \frac{k_0}{k_\perp}}, \quad (12)$$

and the quark gluon vertex is  $gv_i(\lambda^a/2)$ . Higher order corrections can be found by expanding the quark and gluon propagators as well as the HDL vertices in powers of the small parameter  $\epsilon \equiv (k_0/m)$ .

We will refer to the regime in which all momenta, including external ones, satisfy the scaling relation (10) as the Landau damping regime. The Landau damping regime is completely perturbative, i.e. graphs with extra loops are always suppressed by extra powers of  $\epsilon^{1/3}$ . Every quark propagator scales as  $\epsilon^{-2/3}$ , gluon propagators scale as  $\epsilon^{-2/3}$ , and every loop integral gives  $\epsilon^{7/3}$ . The quark-gluon vertex scales as  $\epsilon^0$  and the HDL three-gluon vertex scales as  $\epsilon^{1/3}$ . Using these results we can show that additional loops always increase the power of  $\epsilon^{1/3}$  associated with the diagram.

The effective theory describes a non-Fermi liquid. This is clear from the appearance of fractional powers and logarithms in the low energy expansion. The simplest diagram which gives a logarithmic term is the fermion self energy. We find 15,16,17,18

$$\Sigma(p) = \frac{g^2}{9\pi^2} \left( p_0 \log \left( \frac{2^{5/2}m}{\pi|p_0|} \right) + p_0 + i\frac{\pi}{2}p_0 \right) + O(\epsilon^{5/3}). \quad (13)$$

The scale inside the logarithm is determined by matching the effective theory in the Landau damping regime to an effective theory that contains electric gluon exchanges. The  $p_0 \log(p_0)$  term leads to a vanishing Fermi velocity as we approach the Fermi surface.

The effective theory can also be used to study other higher order corrections. We find, in particular, a QCD version of Migdal's theorem: In the Landau damping regime loop corrections to the quark-gluon vertex are suppressed by powers of  $\epsilon^{1/3}$ .

### 2.3. Color superconductivity

It is well known that the particle-particle scattering amplitude in the BCS channel  $q(\vec{p}) + q(-\vec{p}) \rightarrow q(\vec{p}') + q(-\vec{p}')$  is special. The total momentum of the pair vanishes and as a consequence loop corrections to the scattering amplitude are logarithmically divergent. This implies that all ladder diagrams have to be summed. Crossed ladders, vertex corrections, etc. are perturbative and follow the scaling rules discussed in the previous section.

If the interaction in the particle-particle channel is attractive then the BCS singularity leads to the formation of a pair condensate and to a gap in the fermion spectrum. The gap can be computed by solving a Dyson-Schwinger equation for the anomalous (particle-particle) self energy. In QCD the interaction is attractive in the color anti-triplet channel. The structure of the gap is simplest in the case of two flavors. In that case, there is a unique color anti-symmetric spin zero gap term of the form

$$\langle \psi_i^a C \gamma_5 \psi_j^b \rangle \sim \Delta \epsilon^{3ab} \epsilon^{ij}. \quad (14)$$

Here,  $a, b$  labels color and  $i, j$  flavor. The gap equation is given by 19,20,21,22

$$\Delta(p_4) = \frac{g^2}{18\pi^2} \int dq_4 \log \left( \frac{\Lambda_{BCS}}{|p_4 - q_4|} \right) \frac{\Delta(q_4)}{\sqrt{q_4^2 + \Delta(q_4)^2}}, \quad (15)$$

where the scale  $\Lambda_{BCS} = 256\pi^4(2/N_f)^{5/2}g^{-5}\mu$  is again determined by electric gluon exchanges. The solution to the equation was found by Son<sup>19</sup>. The value of the gap on the Fermi surface  $\Delta_0 = \Delta(p_0=0)$  is

$$\Delta_0 \simeq 2\Lambda_{BCS} \exp\left(-\frac{\pi^2 + 4}{8}\right) \exp\left(-\frac{3\pi^2}{\sqrt{2}g}\right). \quad (16)$$

This result is correct up to  $O(g)$  corrections to the pre-exponent. In order to achieve this accuracy the  $g^2\omega \log(\omega)$  term in the normal self energy, equ. (13), has to be included in the gap equation<sup>23,24,25</sup>. The condensation energy is given by

$$\epsilon = -N_d \Delta_0^2 \left(\frac{\mu^2}{4\pi^2}\right), \quad (17)$$

where  $N_d = 4$  is the number of condensed species.

The situation is slightly more complicated in QCD with  $N_f = 3$  massless flavors. One possibility is to embed the  $N_f = 2$  order parameter into  $N_f = 3$  QCD. This option is usually called the 2SC phase. The energetically preferred phase is the CFL phase described by the order parameter given in equ. (1). In the CFL phase there are eight fermions with gap  $\Delta_{CFL}$  and one fermion with gap  $2\Delta_{CFL}$ . The value of the gap in the CFL phase is smaller than the one in the 2SC phase by a factor<sup>2</sup>  $2^{-1/3}$ . The condensation energy in the two phases is given by

$$\epsilon = -\Delta_0^2 \left(\frac{\mu^2}{4\pi^2}\right) \begin{cases} 4 & \text{2SC} \\ 12 \cdot 2^{-2/3} & \text{CFL} \end{cases} \quad (18)$$

and the CFL phase is preferred by a factor  $(27/4)^{1/3} \simeq 1.89$ .

#### 2.4. Mass terms

Mass terms modify the parameters in the effective lagrangian. These parameters include the Fermi velocity, the effective chemical potential, the screening mass, the BCS terms and the Landau parameters. At tree level the correction to the Fermi velocity and the chemical potential are given by

$$v_F = 1 - \frac{m^2}{2p_F^2}, \quad \delta\mu = -\frac{m^2}{2p_F}. \quad (19)$$

The shift in the Fermi velocity also affects the coupling  $gv_F$  of a magnetic gluon to quarks. It is important to note that at leading order in  $g$  this the only mass correction to the coupling. This is not entirely obvious, as one can imagine a process in which the quark emits a gluon, makes a transition to a virtual high energy state, and then couples back to a low energy state by a mass insertion. This process would give an  $O(m/\mu)$  correction to  $g$ , but it vanishes in the forward direction<sup>26</sup>.

Quark masses modify quark-quark scattering amplitudes and the corresponding Landau and BCS type four-fermion operators. Consider quark-quark scattering in the forward direction,  $v + v' \rightarrow v + v'$ . At tree level in QCD this process receives contribution from the direct and exchange graph. In the effective theory the direct

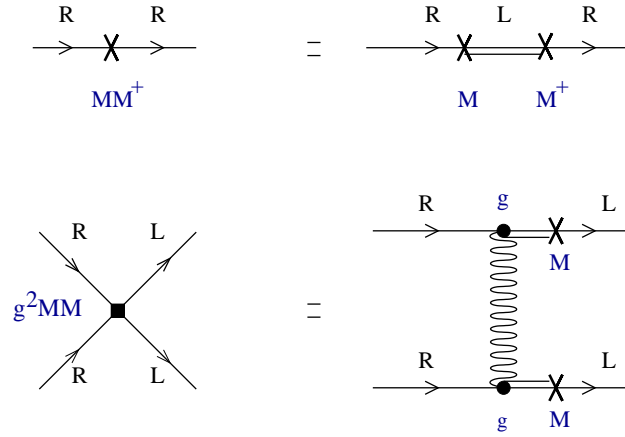


Fig. 2. Mass terms in the high density effective theory. The first diagram shows a  $O(MM^\dagger)$  term that arises from integrating out the  $\psi_-$  field in the QCD lagrangian. The second diagram shows a  $O(M^2)$  four-fermion operator which arises from integrating out  $\psi_-$  and hard gluon exchanges.

term is reproduced by the collinear interaction while the exchange terms has to be matched against a four-fermion operator. The spin-color-flavor symmetric part of the exchange amplitude is given by

$$\mathcal{M}(v, v'; v, v') = \frac{C_F}{4N_c N_f} \frac{g^2}{p_F^2} \left\{ 1 - \frac{m^2}{p_F^2} \frac{x}{1-x} \right\} \quad (20)$$

where  $C_F = (N_c^2 - 1)/(2N_c)$  and  $x = \hat{v} \cdot \hat{v}'$  is the scattering angle. We observe that the amplitude is independent of  $x$  in the limit  $m \rightarrow 0$ . Mass corrections are singular as  $x \rightarrow 1$ . This means that the Landau coefficients  $F_l$  contain logarithms of the cutoff. We note that there is one linear combination of Landau coefficients,  $F_0 - F_1/3$ , which is cutoff independent.

Equations (19-20) are valid for  $N_f \geq 1$  degenerate flavors. Spin and color anti-symmetric BCS amplitudes require at least two different flavors. Consider BCS scattering  $v + (-v) \rightarrow v' + (-v')$  in the helicity flip channel  $L + L \rightarrow R + R$ . The color-anti-triplet amplitude is given by

$$\mathcal{M}(v, -v; v', -v') = \frac{C_A}{4} \frac{g^2}{p_F^2} \frac{m_1 m_2}{p_F^2}. \quad (21)$$

where  $m_1$  and  $m_2$  are the masses of the two quarks and  $C_A = (N_c + 1)/(2N_c)$ . We observe that the scattering amplitude is independent of the scattering angle. This means that at leading order in  $g$  and  $m$  only the s-wave potential  $V_0$  is non-zero.

In order to match Green functions in the high density effective theory to an effective chiral theory of the CFL phase we need to generalize our results to a complex mass matrix of the form  $\mathcal{L} = -\bar{\psi}_L M \psi_R - \bar{\psi}_R M^\dagger \psi_L$ , see Fig. 2. The  $\delta\mu$

term is

$$\mathcal{L} = -\frac{1}{2p_F} \left( \psi_{L+}^\dagger M M^\dagger \psi_{L+} + \psi_{R+}^\dagger M^\dagger M \psi_{R+} \right). \quad (22)$$

and the four-fermion operator in the BCS channel is

$$\begin{aligned} \mathcal{L} = \frac{g^2}{64p_F^4} (\psi_L^{A\dagger} C \psi_L^{B\dagger}) (\psi_R^C C \psi_R^D) & \left\{ \text{Tr} [\lambda^A M (\lambda^D)^T \lambda^B M (\lambda^C)^T] \right. \\ & \left. - \frac{1}{3} \text{Tr} [\lambda^A M (\lambda^D)^T] \text{Tr} [\lambda^B M (\lambda^C)^T] \right\}. \end{aligned} \quad (23)$$

Here, we have introduced the CFL eigenstates  $\psi^A$  defined by  $\psi_i^a = \psi^A (\lambda^A)_{ai} / \sqrt{2}$ ,  $A = 0, \dots, 8$ .

## 2.5. Normal quark matter

Before we consider quark mass effects in the superconducting phase we would like to review mass corrections in the normal phase of quark matter. We will consider three flavor quark matter with massless up and down quarks and massive strange quarks. There are some simple mass effects that we can directly deduce from equ. (19). The strange quark chemical potential is shifted by  $\delta\mu_s = m_s^2 / (2p_F)$  with respect to the strange quark Fermi momentum, and the strange quark Fermi velocity is smaller than one.

It would seem that perturbative corrections to these results are sensitive to momenta far away from the Fermi surface and cannot be computed in the framework of an effective field theory for modes near  $p_F$ . Landau showed, however, that Galilei invariance leads to a relation between the chemical potential and the Fermi momentum that only involves the interaction on the Fermi surface. This relation was generalized to relativistic systems by Baym and Chin<sup>27</sup>. They showed that

$$\mu d\mu = \left[ p_F + \frac{p_F^2}{\pi^2} \left( F_0^s - \frac{1}{3} F_1^s \right) \mu \right] dp_F, \quad (24)$$

where  $F_{0,1}^s$  are color-flavor-spin symmetric Landau coefficients. We observe that this relation involves precisely the combination of Landau coefficients that does not depend on the EFT cutoff. This implies that we can integrate equ. (24) as in ordinary Landau Fermi Liquid theory. The result can be used to determine to thermodynamic potential to  $O(g^2)$ . We get<sup>28,29</sup>

$$\begin{aligned} \Omega = -\frac{N_c}{12\pi^2} & \left[ \mu u (\mu^2 - \frac{5}{2} m^2) + \frac{3}{2} m^4 \ln \left( \frac{\mu + u}{m} \right) \right] \\ & + \frac{\alpha_s (N_c^2 - 1)}{16\pi^3} \left[ 3 \left( m^2 \ln \frac{\mu + u}{m} - \mu u \right)^2 - 2u^4 \right]. \end{aligned} \quad (25)$$

with  $u = \sqrt{\mu^2 - m^2}$ . This result corresponds to a momentum space subtraction scheme. The thermodynamic potential in the  $\overline{MS}$  scheme was computed by

Fraga and Romatschke<sup>30</sup>. Perturbative corrections reduce the pressure of a quark gas. The same is true for mass corrections to the pressure in the non-interacting system. The  $O(\alpha_s m^2)$  term, however, increases the pressure. This is related to the fact that the exchange energy in a degenerate quark gas changes sign in going from the non-relativistic limit, dominated by the Coulomb interaction, to the relativistic system in which magnetic interactions are more important.

In applications to neutron stars we have to include weak interactions and enforce electric charge neutrality. Weak interactions can convert strange quarks into up quarks, electrons and neutrinos. We will assume that neutrinos can leave the system. Under these assumptions the system is characterized by a baryon chemical potential  $\mu$  and an electron chemical potential  $\mu_e$ . The electron chemical potential is fixed by the condition of electric charge neutrality,  $(\partial\Omega)/(\partial\mu_e) = 0$ .

To leading order in  $m_s^2/p_F^2$  the electron chemical potential is given by

$$\mu_e \simeq \frac{m_s^2}{4p_F} \left( 1 - \frac{4\alpha_s}{\pi} \log \left( \frac{2p_F}{m_s} \right) \right). \quad (26)$$

At tree level we find  $\mu_e = \mu_s/2$  and the Fermi surfaces are split symmetrically

$$p_F^d = p_F^u + \mu_s/2, \quad p_F^s = p_F^u - \mu_s/2. \quad (27)$$

Perturbative corrections reduce the magnitude of  $\mu_e$ . In fact, since the  $O(\alpha_s)$  term is enhanced by a large logarithm  $\log(p_F/m)$ , the electron chemical potential can become negative. This result is probably not reliable. In particular, the  $O(\alpha_s)$  term is modified if the  $\overline{MS}$  mass is used.

### 3. Chiral theory of the CFL phase

#### 3.1. Introduction

The main topic of this review is the effect of the strange quark mass on the CFL phase. In principle this problem can be studied by solving a gap equations which includes mass corrections to the chemical potential, the Fermi velocity, and the quark-quark interaction. In full QCD this has not been attempted yet, but there are many calculations of this type that are based on effective four-fermion models of QCD. We will compare our results with some of these calculations in Sect. 3.8.

There are several difficulties with microscopic calculations of this kind. The first is that they typically require an ansatz for the gap parameter. We will see that both flavor symmetry and isospin are broken, and that the gaps for the left and right handed fermions acquire a relative phase. This means that the number of independent gap parameters is quite large. The second difficulty is that while the ideal CFL state is automatically neutral with respect to all charges, this is no longer the case once the state is perturbed by a finite strange quark mass. This means that we have to introduce flavor chemical potentials and gluonic background fields. Finally, we know that chiral symmetry is broken in the CFL phase and this implies that physical observables are non-analytic in the quark mass.

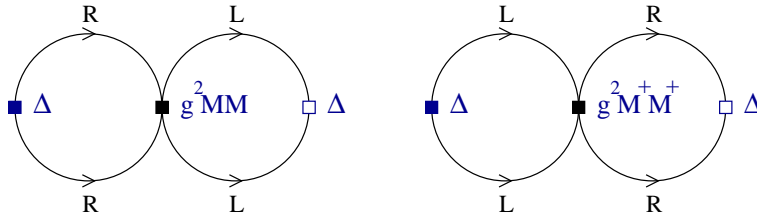


Fig. 3. Contribution of the  $O(M^2)$  BCS four-fermion operator to the condensation energy in the CFL phase .

These non-analyticities are related to Goldstone bosons. This suggests that we should study the effects of a non-zero strange quark mass using an effective field theory for the Goldstone modes. Indeed, it is well known that chiral symmetry places important constraints on the mass dependence of QCD observables, and that these constraints are most easily implemented by using an effective lagrangian.

### 3.2. Chiral effective field theory

For excitation energies smaller than the gap the only relevant degrees of freedom are the Goldstone modes associated with the breaking of chiral symmetry and baryon number. Since the pattern of chiral symmetry breaking is identical to the one at  $T = \mu = 0$  the effective lagrangian has the same structure as chiral perturbation theory. The main difference is that Lorentz-invariance is broken and only rotational invariance is a good symmetry. The effective lagrangian for the Goldstone modes is given by <sup>31</sup>

$$\begin{aligned} \mathcal{L}_{eff} = & \frac{f_\pi^2}{4} \text{Tr} [\nabla_0 \Sigma \nabla_0 \Sigma^\dagger - v_\pi^2 \partial_i \Sigma \partial_i \Sigma^\dagger] + [B \text{Tr}(M \Sigma^\dagger) + h.c.] \\ & + [A_1 \text{Tr}(M \Sigma^\dagger) \text{Tr}(M \Sigma^\dagger) + A_2 \text{Tr}(M \Sigma^\dagger M \Sigma^\dagger) \\ & + A_3 \text{Tr}(M \Sigma^\dagger) \text{Tr}(M^\dagger \Sigma) + h.c.] + \dots \end{aligned} \quad (28)$$

Here  $\Sigma = \exp(i\phi^a \lambda^a / f_\pi)$  is the chiral field,  $f_\pi$  is the pion decay constant and  $M$  is a complex mass matrix. The chiral field and the mass matrix transform as  $\Sigma \rightarrow L \Sigma R^\dagger$  and  $M \rightarrow L M R^\dagger$  under chiral transformations  $(L, R) \in SU(3)_L \times SU(3)_R$ . We have suppressed the singlet fields associated with the breaking of the exact  $U(1)_V$  and approximate  $U(1)_A$  symmetries.

At low density the coefficients  $f_\pi, B, A_i, \dots$  are non-perturbative quantities that have to be extracted from experiment or measured on the lattice. At large density, on the other hand, the chiral coefficients can be calculated in perturbative QCD. For the derivative terms this is most easily done by matching the two-point functions of flavor currents between QCD and the chiral theory. The mass terms can be computed by matching the mass dependence of the vacuum energy. At leading

order in  $\alpha_s$  the Goldstone boson decay constant and velocity are <sup>32</sup>

$$f_\pi^2 = \frac{21 - 8 \log(2)}{18} \left( \frac{p_F^2}{2\pi^2} \right), \quad v_\pi^2 = \frac{1}{3}. \quad (29)$$

Mass terms are determined by the operators studied in Sect. 2.4. We observe that both equ. (22) and (23) are quadratic in  $M$ . This implies that  $B = 0$  in perturbative QCD.  $B$  receives non-perturbative contributions from instantons, but these effects are small if the density is large, see Sect. 3.7.

We observe that  $X_L = MM^\dagger/(2p_F)$  and  $X_R = M^\dagger M/(2p_F)$  in equ. (22) act as effective chemical potentials for left and right-handed fermions, respectively. Formally, the effective lagrangian has an  $SU(3)_L \times SU(3)_R$  gauge symmetry under which  $X_{L,R}$  transform as the temporal components of non-abelian gauge fields. We can implement this approximate gauge symmetry in the CFL chiral theory by promoting time derivatives to covariant derivatives <sup>33</sup>,

$$\nabla_0 \Sigma = \partial_0 \Sigma + i \left( \frac{MM^\dagger}{2p_F} \right) \Sigma - i \Sigma \left( \frac{M^\dagger M}{2p_F} \right). \quad (30)$$

The BCS four-fermion operator in equ. (23) contributes to the condensation energy in the CFL phase, see Fig. 3. We find <sup>32,26</sup>

$$\Delta \mathcal{E} = -\frac{3\Delta^2}{4\pi^2} \left\{ \left( \text{Tr}[M] \right)^2 - \text{Tr}[M^2] \right\} + (M \leftrightarrow M^\dagger). \quad (31)$$

This term can be matched against the  $A_i$  terms in the effective lagrangian. The result is <sup>32,26</sup>

$$A_1 = -A_2 = \frac{3\Delta^2}{4\pi^2}, \quad A_3 = 0. \quad (32)$$

The vacuum energy also receives contributions from Landau-type four-fermion operators, but these terms are proportional to  $\text{Tr}[MM^\dagger]$  and do not depend on the chiral field  $\Sigma$ .

We can now summarize the structure of the chiral expansion in the CFL phase. The effective lagrangian has the form

$$\mathcal{L} \sim f_\pi^2 \Delta^2 \left( \frac{\partial_0}{\Delta} \right)^k \left( \frac{\vec{\partial}}{\Delta} \right)^l \left( \frac{MM^\dagger}{p_F \Delta} \right)^m \left( \frac{MM}{p_F^2} \right)^n (\Sigma)^o (\Sigma^\dagger)^p. \quad (33)$$

Loop graphs in the effective theory are suppressed by powers of  $\partial/(4\pi f_\pi)$ . Since the pion decay constant scales as  $f_\pi \sim p_F$  Goldstone boson loops are suppressed compared to higher order contact terms. We also note that the quark mass expansion is controlled by  $m^2/(p_F \Delta)$ . This means that the chiral expansion breaks down if  $m^2 \sim p_F \Delta$ . This is the same scale at which BCS calculations find a transition from the CFL phase to a less symmetric state.

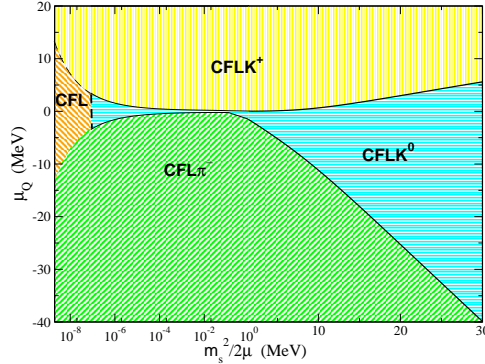


Fig. 4. Phase structure of CFL matter as a function of the effective chemical potential  $\mu_s = m_s^2/(2p_F)$  and the lepton chemical potential  $\mu_Q$ , from Kaplan & Reddy (2001). A typical value of  $\mu_s$  in a neutron star is 10 MeV.

### 3.3. Kaon condensation

Using the chiral effective lagrangian we can now determine the dependence of the order parameter on the quark masses. We will focus on the physically relevant case  $m_s > m_u = m_d$ . Because the main expansion parameter is  $m_s^2/(p_F\Delta)$  increasing the quark mass is roughly equivalent to lowering the density. The effective potential for the order parameter is

$$V_{eff} = \frac{f_\pi^2}{4} \text{Tr} [2X_L \Sigma X_R \Sigma^\dagger - X_L^2 - X_R^2] - A_1 \left[ (\text{Tr}(M\Sigma^\dagger))^2 - \text{Tr}((M\Sigma^\dagger)^2) \right]. \quad (34)$$

The first term contains the effective chemical potential  $\mu_s = m_s^2/(2p_F)$  and favors states with a deficit of strange quarks (with strangeness  $S = -1$ ). The second term favors the neutral ground state  $\Sigma = 1$ . The lightest excitation with positive strangeness is the  $K^0$  meson. We therefore consider the ansatz  $\Sigma = \exp(i\alpha\lambda_4)$  which allows the order parameter to rotate in the  $K^0$  direction. The vacuum energy is

$$V(\alpha) = -f_\pi^2 \left( \frac{1}{2} \left( \frac{m_s^2 - m^2}{2p_F} \right)^2 \sin^2(\alpha) + (m_K^0)^2 (\cos(\alpha) - 1) \right), \quad (35)$$

where  $(m_K^0)^2 = (4A_1/f_\pi^2)m(m + m_s)$ . Minimizing the vacuum energy we obtain

$$\cos(\alpha) = \begin{cases} 1 & \mu_s < m_K^0 \\ \frac{(m_K^0)^2}{\mu_s^2} & \mu_s > m_K^0 \end{cases} \quad (36)$$

The hypercharge density is

$$n_Y = f_\pi^2 \mu_s \left( 1 - \frac{(m_K^0)^4}{\mu_s^4} \right). \quad (37)$$

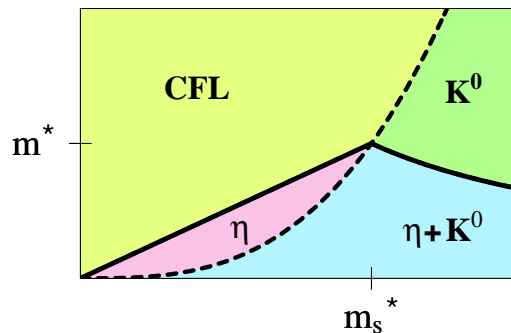


Fig. 5. Phase structure of CFL matter as a function of the light quark mass  $m$  and the strange quark mass  $m_s$ , from Kryjevski, Kaplan & Schäfer (2005).

This result has the same structure as the charge density of a weakly interacting Bose condensate. Using the perturbative result for  $A_1$  we can get an estimate of the critical strange quark mass. We find

$$m_s(\text{crit}) = 3.03 \cdot m_d^{1/3} \Delta^{2/3}, \quad (38)$$

from which we obtain  $m_s(\text{crit}) \simeq 70$  MeV for  $\Delta \simeq 50$  MeV. This result suggests that strange quark matter at densities that can be achieved in neutron stars is kaon condensed. We also note that the difference in condensation energy between the CFL phase and the kaon condensed state is not necessarily small. For  $\mu_s \rightarrow \Delta$  we have  $\sin(\alpha) \rightarrow 1$  and  $V(\alpha) \rightarrow f_\pi^2 \Delta^2 / 2$ . Since  $f_\pi^2$  is of order  $\mu^2 / (2\pi^2)$  this is comparable to the condensation energy in the CFL phase.

The strange quark mass breaks the  $SU(3)$  flavor symmetry to  $SU(2)_I \times U(1)_Y$ . In the kaon condensed phase this symmetry is spontaneously broken to  $U(1)_Q$ . If isospin is an exact symmetry there are two exactly massless Goldstone modes<sup>34</sup>, the  $K^0$  and the  $K^+$ . Isospin breaking leads to a small mass for the  $K^+$ . The phase structure as a function of the strange quark mass and non-zero lepton chemical potentials was studied by Kaplan and Reddy<sup>35</sup>, see Fig. 4. We observe that if the lepton chemical potential is non-zero charged kaon and pion condensates are also possible.

### 3.4. Eta meson condensation

The CFL phase also contains a very light  $S = 0$  mode which can potentially become unstable. This mode is a linear combination of the  $\eta$  and  $\eta'$  and its mass is proportional to  $m_u m_d$ . Because this mode has zero strangeness it is not affected by the  $\mu_s$  term in the effective potential. However, since  $m_u, m_d \ll m_s$  this state is sensitive to perturbative  $\alpha_s m_s^2$  corrections. The relevant contribution to the effective lagrangian is<sup>36</sup>

$$\delta\mathcal{L} = -\delta A \left[ (\text{Tr} M \Sigma^\dagger)^2 + \text{Tr} (M \Sigma^\dagger)^2 \right] + \text{h.c.}, \quad (39)$$

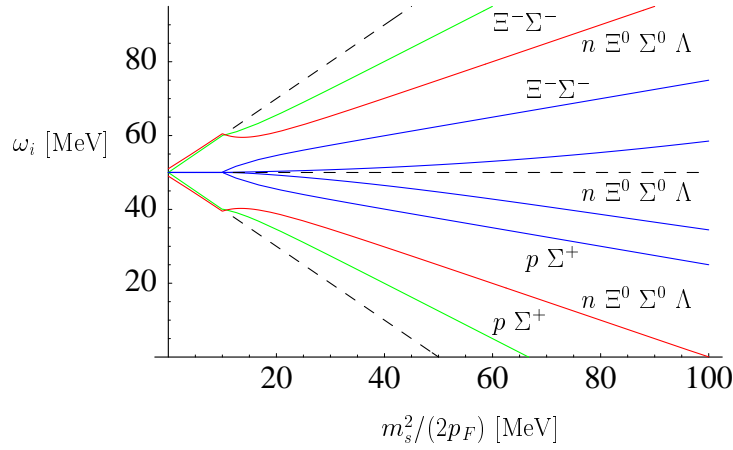


Fig. 6. This figure shows the fermion spectrum in the CFL phase. For  $m_s = 0$  there are eight fermions with gap  $\Delta$  and one fermion with gap  $2\Delta$  (not shown). Without kaon condensation gapless fermion modes appear at  $\mu_s = \Delta$  (dashed lines). With kaon condensation gapless modes appear at  $\mu_s = 4\Delta/3$ .

with

$$\delta A = \frac{3}{8\pi^2} \Delta_6^2, \quad \Delta_6^2 = \alpha_s \frac{(\ln 2)^2}{162\pi} \Delta^2. \quad (40)$$

Here,  $\Delta_6$  is a color-flavor symmetric gap parameter which is generated by perturbative corrections to the dominant, color-flavor anti-symmetric gap  $^2$ . Since the one-gluon exchange interaction in the color-symmetric channel is repulsive the  $O(\alpha_s m_s^2)$  contribution to the mass of the  $\eta - \eta'$  mode tends to cancel the  $O(m_u m_d)$  term. When the two terms become equal the eta condenses. The resulting phase diagram is shown in Fig. 5. The precise value of the tetra-critical point  $(m^*, m_s^*)$  depends sensitively on the value of the coupling constant. At very high density  $m^*$  is extremely small, but at moderate density  $m^*$  can become as large as 5 MeV, comparable to the physical values of the up and down quark mass.

### 3.5. Fermions in the CFL phase

So far we have only studied Goldstone modes in the CFL phase. However, as the strange quark mass is increased it is possible that some of the fermion modes become light or even gapless  $^{37}$ . In order to study this question we have to include fermions in the effective field theory. The effective lagrangian for fermions in the CFL phase is  $^{38,39}$

$$\begin{aligned} \mathcal{L} = & \text{Tr} (N^\dagger i v^\mu D_\mu N) - D \text{Tr} (N^\dagger v^\mu \gamma_5 \{ \mathcal{A}_\mu, N \}) - F \text{Tr} (N^\dagger v^\mu \gamma_5 [ \mathcal{A}_\mu, N ]) \\ & + \frac{\Delta}{2} \left\{ \left( \text{Tr} (N_L N_L) - [\text{Tr} (N_L)]^2 \right) - (L \leftrightarrow R) + h.c. \right\}. \end{aligned} \quad (41)$$

$N_{L,R}$  are left and right handed baryon fields in the adjoint representation of flavor  $SU(3)$ . The baryon fields originate from quark-hadron complementarity<sup>40</sup>. We can think of  $N$  as describing a quark which is surrounded by a diquark cloud,  $N_L \sim q_L \langle q_L q_L \rangle$ . The covariant derivative of the nucleon field is given by  $D_\mu N = \partial_\mu N + i[\mathcal{V}_\mu, N]$ . The vector and axial-vector currents are

$$\mathcal{V}_\mu = -\frac{i}{2} \{ \xi \partial_\mu \xi^\dagger + \xi^\dagger \partial_\mu \xi \}, \quad \mathcal{A}_\mu = -\frac{i}{2} \xi (\nabla_\mu \Sigma^\dagger) \xi, \quad (42)$$

where  $\xi$  is defined by  $\xi^2 = \Sigma$ . It follows that  $\xi$  transforms as  $\xi \rightarrow L \xi U(x)^\dagger = U(x) \xi R^\dagger$  with  $U(x) \in SU(3)_V$ . For pure  $SU(3)$  flavor transformations  $L = R = V$  we have  $U(x) = V$ .  $F$  and  $D$  are low energy constants that determine the baryon axial coupling. In perturbative QCD we find  $D = F = 1/2$ .

The effective theory given in equ. (41) can be derived from QCD in the weak coupling limit. However, the structure of the theory is completely determined by chiral symmetry, even if the coupling is not weak. In particular, there are no free parameters in the baryon coupling to the vector current. Mass terms are also strongly constrained by chiral symmetry. The effective chemical potentials  $(X_L, X_R)$  appear as left and right-handed gauge potentials in the covariant derivative of the nucleon field. We have

$$D_0 N = \partial_0 N + i[\Gamma_0, N], \quad (43)$$

$$\Gamma_0 = -\frac{i}{2} \{ \xi (\partial_0 + iX_R) \xi^\dagger + \xi^\dagger (\partial_0 + iX_L) \xi \},$$

where  $X_L = MM^\dagger/(2p_F)$  and  $X_R = M^\dagger M/(2p_F)$  as before.  $(X_L, X_R)$  covariant derivatives also appears in the axial vector current given in equ. (42).

We can now study how the fermion spectrum depends on the quark mass. In the CFL state we have  $\xi = 1$ . For  $\mu_s = 0$  the baryon octet has an energy gap  $\Delta$  and the singlet has gap  $2\Delta$ . As a function of  $\mu_s$  the excitation energy of the proton and neutron is lowered,  $\omega_{p,n} = \Delta - \mu_s$ , while the energy of the cascade states  $\Xi^-, \Xi^0$  particles is raised,  $\omega_\Xi = \Delta + \mu_s$ . All other excitation energies are independent of  $\mu_s$ . As a consequence we find gapless  $(p, n)$  and  $(\Xi^-, \Xi^0)^{-1}$  excitations at  $\mu_s = \Delta$ .

The situation is more complicated when kaon condensation is taken into account. In the kaon condensed phase there is mixing in the  $(p, \Sigma^+, \Sigma^-, \Xi^-)$  and  $(n, \Sigma^0, \Xi^0, \Lambda^8, \Lambda^0)$  sector. For  $m_K^0 \ll \mu_s \ll \Delta$  the spectrum is given by

$$\omega_{p\Sigma^\pm \Xi^-} = \begin{cases} \Delta \pm \frac{3}{4}\mu_s, \\ \Delta \pm \frac{1}{4}\mu_s, \end{cases} \quad \omega_{n\Sigma^0 \Xi^0 \Lambda} = \begin{cases} \Delta \pm \frac{1}{2}\mu_s, \\ \Delta, \\ 2\Delta. \end{cases} \quad (44)$$

Numerical results for the eigenvalues are shown in Fig. 6. We observe that mixing within the charged and neutral baryon sectors leads to level repulsion. There are two modes that become light in the CFL window  $\mu_s \leq 2\Delta$ . One mode is a linear combination of proton and  $\Sigma^+$  particles, as well as  $\Xi^-$  and  $\Sigma^-$  holes, and the other mode is a linear combination of the neutral baryons  $(n, \Sigma^0, \Xi^0, \Lambda^8, \Lambda^0)$ .

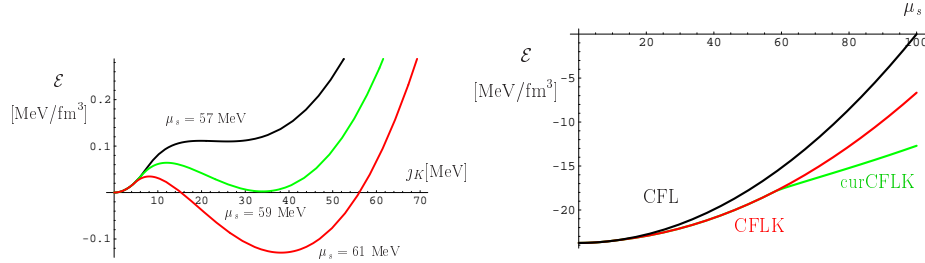


Fig. 7. Left panel: Energy density as a function of the current  $J_K$  for several different values of  $\mu_s = m_s^2/(2p_F)$  close to the phase transition. Right panel: Ground state energy density as a function of  $\mu_s$ . We show the CFL phase, the kaon condensed CFL (KCFL) phase, and the supercurrent state (curKCFL).

### 3.6. Meson supercurrent state

Recently, several groups have shown that gapless fermion modes lead to instabilities in the current-current correlation function<sup>41,42</sup>. Motivated by these results we have examined the stability of the kaon condensed phase against the formation of a non-zero current<sup>43,44</sup>. Consider a spatially varying  $U(1)_Y$  rotation of the maximal kaon condensate

$$U(x)\xi_{K^0}U^\dagger(x) = \begin{pmatrix} 1 & 0 & 0 \\ 0 & 1/\sqrt{2} & ie^{i\phi_K(x)}/\sqrt{2} \\ 0 & ie^{-i\phi_K(x)}/\sqrt{2} & 1/\sqrt{2} \end{pmatrix}. \quad (45)$$

This state is characterized by non-zero currents

$$\vec{V} = \frac{1}{2} (\vec{\nabla}\phi_K) \begin{pmatrix} 0 & 0 & 0 \\ 0 & 1 & 0 \\ 0 & 0 & -1 \end{pmatrix}, \quad \vec{A} = \frac{1}{2} (\vec{\nabla}\phi_K) \begin{pmatrix} 0 & 0 & 0 \\ 0 & 0 & -ie^{i\phi_K} \\ 0 & ie^{-i\phi_K} & 0 \end{pmatrix}. \quad (46)$$

In the following we compute the vacuum energy as a function of the kaon current  $\vec{J}_K = \vec{\nabla}\phi_K$ . The meson part of the effective lagrangian gives a positive contribution

$$\mathcal{E} = \frac{1}{2} v_\pi^2 f_\pi^2 J_K^2. \quad (47)$$

A negative contribution can arise from gapless fermions. In order to determine this contribution we have to calculate the fermion spectrum in the presence of a non-zero current. The relevant part of the effective lagrangian is

$$\begin{aligned} \mathcal{L} = & \text{Tr} (N^\dagger i v^\mu D_\mu N) + \text{Tr} (N^\dagger \gamma_5 (\rho_A + \vec{v} \cdot \vec{A}) N) \\ & + \frac{\Delta}{2} \{ \text{Tr} (NN) - \text{Tr} (N) \text{Tr} (N) + h.c. \}, \end{aligned} \quad (48)$$

where we have used  $D = F = 1/2$ . The covariant derivative is  $D_0 N = \partial_0 N + i[\rho_V, N]$  and  $D_i N = \partial_i N + i\vec{v} \cdot [\vec{\mathcal{V}}, N]$  with  $\vec{\mathcal{V}}, \vec{\mathcal{A}}$  given in equ. (46) and

$$\rho_{V,A} = \frac{1}{2} \left\{ \xi \frac{M^\dagger M}{2p_F} \xi^\dagger \pm \xi^\dagger \frac{M M^\dagger}{2p_F} \xi \right\}. \quad (49)$$

The vector potential  $\rho_V$  and the vector current  $\vec{\mathcal{V}}$  are diagonal in flavor space while the axial potential  $\rho_A$  and the axial current  $\vec{\mathcal{A}}$  lead to mixing. The fermion spectrum is quite complicated. The dispersion relation of the lowest mode is approximately given by

$$\omega_l = \Delta + \frac{(l - l_0)^2}{2\Delta} - \frac{3}{4}\mu_s - \frac{1}{4}\vec{v} \cdot \vec{J}_K, \quad (50)$$

where  $l = \vec{v} \cdot \vec{p} - p_F$  and we have expanded  $\omega_l$  near its minimum  $l_0 = (\mu_s + \vec{v} \cdot \vec{J}_K)/4$ . Equation (50) shows that there is a gapless mode if  $\mu_s > 4\Delta/3 - J_K/3$ . The contribution of the gapless mode to the vacuum energy is

$$\mathcal{E} = \frac{\mu^2}{\pi^2} \int dl \int \frac{d\Omega}{4\pi} \omega_l \theta(-\omega_l), \quad (51)$$

where  $d\Omega$  is an integral over the Fermi surface. The integral in equ. (51) receives contributions from one of the pole caps on the Fermi surface. The result has exactly the same structure as the energy functional of a non-relativistic two-component Fermi liquid with non-zero polarization, see Sect. 4. Introducing dimensionless variables

$$x = \frac{J_K}{a\Delta}, \quad h = \frac{3\mu_s - 4\Delta}{a\Delta}. \quad (52)$$

we can write  $\mathcal{E} = c\mathcal{N}f_h(x)$  with

$$f_h(x) = x^2 - \frac{1}{x} \left[ (h+x)^{5/2} \Theta(h+x) - (h-x)^{5/2} \Theta(h-x) \right]. \quad (53)$$

We have defined the constants

$$c = \frac{2}{15^4 c_\pi^3 v_\pi^6}, \quad \mathcal{N} = \frac{\mu^2 \Delta^2}{\pi^2}, \quad a = \frac{2}{15^2 c_\pi^2 v_\pi^4}, \quad (54)$$

where  $c_\pi = (21 - 8 \log(2))/36$  is the numerical coefficient that appears in the weak coupling result for  $f_\pi$ . According to the analysis in <sup>45</sup> the function  $f_h(x)$  develops a non-trivial minimum if  $h_1 < h < h_2$  with  $h_1 \simeq -0.067$  and  $h_2 \simeq 0.502$ . In perturbation theory we find  $a = 0.43$  and the kaon condensed ground state becomes unstable for  $(\Delta - 3\mu_s/4) < 0.007\Delta$ .

The energy density as a function of the current and the groundstate energy density as a function of  $\mu_s$  are shown in Fig. 7. In these plots we have included the contribution of a baryon current  $J_B$ , as suggested in <sup>44</sup>. In this case we have to minimize the energy with respect to two currents. The solution is of the form  $J_B \sim J_K$ . The figure shows the dependence on  $J_K$  for the optimum value of  $J_B$ . We have not properly implemented electric charge neutrality. Since the gapless mode is charged, enforcing electric neutrality will significantly suppress the magnitude of

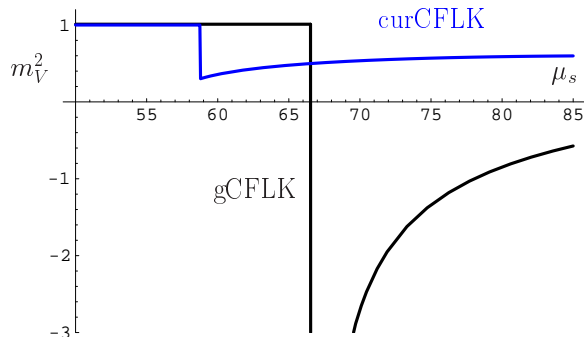


Fig. 8. Screening mass of flavor gauge fields in the CFL phase. The two curves show the second derivative of the effective potential with respect to the current at the origin and at the minimum of the potential.

the current<sup>46</sup>. We have also not included the possibility that the neutral mode becomes gapless. This will happen at somewhat larger values of  $\mu_s$ .

We note that the ground state has no net current. This is clear from the fact that the ground state satisfies  $\delta\mathcal{E}/\delta(\vec{\nabla}\phi_K) = 0$ . As a consequence the meson current is canceled by an equal but opposite contribution from gapless fermions. We also expect that the ground state has no chromomagnetic instabilities. From the effective lagrangian we can compute the screening length of a  $SU(3)_F$  gauge field. In the CFL phase the isospin and hypercharge screening masses are

$$m_V^2 = \left. \frac{\partial^2 \mathcal{E}}{\partial j_K^2} \right|_{j_K=0} = v_\pi^2 f_\pi^2 \left( 1 - \frac{5}{8\sqrt{h}} \theta(h) \right), \quad (55)$$

which shows the magnetic instability for  $h > 0$  and has the characteristic square root singularity observed in microscopic calculations<sup>41</sup>. In Fig. 8 we show the screening mass in the kaon condensed CFL phase and the supercurrent phase as a function of  $\mu_s$ . We observe that there is an instability in the homogeneous phase, but the instability disappears in the supercurrent state.

### 3.7. Instanton effects

The results discussed in Sects. 3.3-3.6 are based on an effective chiral theory of the CFL phase. The coefficients of the effective theory are determined by matching to perturbative QCD calculations. We find that the chiral coefficients are “natural”, i.e. their numerical value agrees with simple dimensional estimates. For example,  $f_\pi^2$  is given, up to a coefficient of order one, by the density of states on the Fermi surface. This suggest that many of our results are valid even if the QCD coupling is not weak.

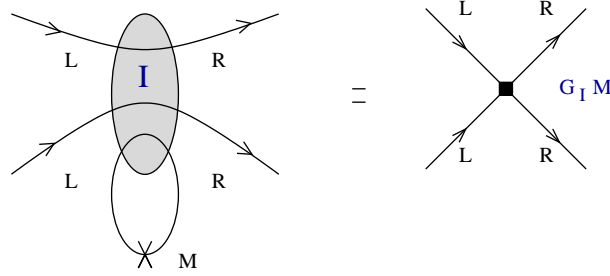


Fig. 9. Instanton contribution to the BCS four-fermion operator in QCD with three flavors.

A possible exception is the linear mass term in the effective chiral theory. The coefficient  $B$  in equ. (28) vanishes to all orders in perturbation theory, but  $B$  receives non-perturbative contributions from instantons. In QCD with three flavors instantons induce a four-fermion operator<sup>47</sup>.

$$\mathcal{L} = \int n(\rho, \mu) d\rho \frac{2(2\pi\rho)^4 \rho^3}{4(N_c^2 - 1)} \epsilon_{f_1 f_2 f_3} \epsilon_{g_1 g_2 g_3} M_{f_3 g_3} \left( \frac{2N_c - 1}{2N_c} (\bar{\psi}_{R, f_1} \psi_{L, g_1}) (\bar{\psi}_{R, f_2} \psi_{L, g_2}) - \frac{1}{8N_c} (\bar{\psi}_{R, f_1} \sigma_{\mu\nu} \psi_{L, g_1}) (\bar{\psi}_{R, f_2} \sigma_{\mu\nu} \psi_{L, g_2}) + (M \leftrightarrow M^\dagger, L \leftrightarrow R) \right), \quad (56)$$

see Fig. 9. Here,  $f_i, g_i$  are flavor indices and  $\sigma_{\mu\nu} = \frac{i}{2}[\gamma_\mu, \gamma_\nu]$ . The instanton size distribution  $n(\rho, \mu)$  is given by

$$n(\rho, \mu) = C_N \left( \frac{8\pi^2}{g^2} \right)^{2N_c} \rho^{-5} \exp \left[ -\frac{8\pi^2}{g(\rho)^2} \right] \exp [-N_f \rho^2 \mu^2], \quad (57)$$

$$C_N = \frac{0.466 \exp(-1.679N_c) 1.34^{N_f}}{(N_c - 1)!(N_c - 2)!}. \quad (58)$$

At zero density, the  $\rho$  integral in equ. (56) diverges for large  $\rho$ . This is the well-known infrared problem of the semi-classical approximation in QCD. At large chemical potential, however, large instantons are suppressed and the typical instanton size is  $\rho \sim \mu^{-1} \ll \Lambda_{QCD}^{-1}$  where  $\Lambda_{QCD}$  is the QCD scale parameter. The instanton contribution to the vacuum energy density is

$$\mathcal{E} = - \int n(\rho, \mu) d\rho \frac{16}{3} (\pi\rho)^4 \rho^3 \left[ \frac{3\sqrt{2}\pi}{g} \Delta \left( \frac{\mu^2}{2\pi^2} \right) \right]^2 \text{Tr} [M + M^\dagger]. \quad (59)$$

This result can be matched against the  $O(M)$  term in the effective chiral lagrangian. We find

$$B = C_N \frac{8\pi^4}{3} \frac{\Gamma(6)}{3^6} \left[ \frac{3\sqrt{2}\pi}{g} \Delta \left( \frac{\mu^2}{2\pi^2} \right) \right]^2 \left( \frac{8\pi^2}{g^2} \right)^6 \left( \frac{\Lambda_{QCD}}{\mu} \right)^{12} \Lambda_{QCD}^{-3}, \quad (60)$$

where we have performed the integral over the instanton size  $\rho$  using the one-loop beta function. The coefficient  $B$  is related to the quark-anti-quark condensate,  $\langle \bar{\psi}\psi \rangle = -2B$ . The linear mass terms contributes to the mass of the kaon,

Table 1. Effective chemical potential for the different quark modes. The quark modes are labeled by their color (rgb) and flavor (uds). We also show the  $\tilde{Q}$  charge and the corresponding baryon mode. The leading order result in the neutral CFL phase corresponds to  $\mu_e = \mu_3 = 0$  and  $\mu_8 = -\mu_s$ .

mode	$\tilde{Q}$	effective chemical potential	leading order	baryon mode
ru	0	$-\frac{2}{3}\mu_e + \frac{1}{2}\mu_3 + \frac{1}{3}\mu_8$	$\mu_0$	
gd	0	$+\frac{1}{3}\mu_e - \frac{1}{2}\mu_3 + \frac{1}{3}\mu_8$	$\mu_0$	$(\Lambda_0, \Lambda_8, \Sigma_0)$
bs	0	$+\frac{1}{3}\mu_e - \frac{2}{3}\mu_8 - \mu_s$	$\mu_0$	
rd	-1	$+\frac{1}{3}\mu_e + \frac{1}{2}\mu_3 + \frac{1}{3}\mu_8$	$\mu_0$	$\Sigma^-$
gu	1	$-\frac{2}{3}\mu_e - \frac{1}{2}\mu_3 + \frac{1}{3}\mu_8$	$\mu_0$	$\Sigma^+$
rs	-1	$+\frac{1}{3}\mu_e + \frac{1}{2}\mu_3 + \frac{1}{3}\mu_8 - \mu_s$	$\mu_0 - \mu_s$	$\Xi^-$
bu	1	$-\frac{2}{3}\mu_e - \frac{2}{3}\mu_8$	$\mu_0 + \mu_s$	$p$
gs	0	$+\frac{1}{3}\mu_e - \frac{1}{2}\mu_3 + \frac{1}{3}\mu_8 - \mu_s$	$\mu_0 - \mu_s$	$\Xi^0$
bd	0	$+\frac{1}{3}\mu_e - \frac{2}{3}\mu_8$	$\mu_0 + \mu_s$	$n$

$\delta m_K^2 \sim (4B/f_\pi^2)mm_s$ , and tends to inhibit kaon condensation. At moderate density this contribution is quite uncertain because the result is very sensitive to the value of the strong coupling constant. Using the one-loop running coupling and  $\Lambda_{QCD} \simeq 200$  MeV gives values as large as  $\delta m_K \sim 100$  MeV. This is almost certainly an overestimate because the main contribution comes from large instantons with size  $\rho \sim 0.5$  fm. If the average instanton size is constrained to be less than the phenomenological value at zero density,  $\bar{\rho} = 0.35$  fm, then we find  $\delta m_K < 10$  MeV.

### 3.8. Microscopic models

In this section we shall compare some of our results with microscopic calculations based on Nambu-Jona-Lasinio (NJL) models, see for example <sup>37,48</sup>. A natural choice is to model the interaction between quarks by a local four-fermion interaction with the quantum numbers of one-gluon exchange

$$\mathcal{L} = \bar{\psi} (i\cancel{D} + \mu\gamma_0 - M) \psi + G (\bar{\psi}\gamma_\mu\lambda^a\psi)^2. \quad (61)$$

This lagrangian has the symmetries of QCD except that the  $SU(3)$  color symmetry is global rather than local, and the axial  $U(1)_A$  is not anomalous. The effects of the anomaly can be taken into account by adding the instanton induced four-fermion interaction given in equ. (56). Since color is a global symmetry the NJL model does not exhibit a Higgs mechanism and color superconductivity leads to an extra octet of colored Goldstone bosons.

The pairing ansatz is usually taken to be

$$\langle \psi_i^a C \gamma_5 \psi_j^b \rangle \sim \Delta_1 \epsilon^{ab1} \epsilon_{ij1} + \Delta_2 \epsilon^{ab2} \epsilon_{ij2} + \Delta_3 \epsilon^{ab3} \epsilon_{ij3}. \quad (62)$$

This ansatz reduces to the CFL ansatz for  $\Delta_1 = \Delta_2 = \Delta_3$  and allows for the breaking of hypercharge and isospin. The ansatz is not sufficiently rich to allow for

kaon condensation. The chiral field  $\Sigma$  can be defined as

$$\Sigma = XY^\dagger, \quad (63)$$

where  $X, Y$  are related to the left and right handed condensates

$$\langle (\psi_L)_i^a C(\psi_L)_j^b \rangle \epsilon^{abc} \epsilon_{ijk} \sim X_k^c, \quad (64)$$

$$\langle (\psi_R)_i^a C(\psi_R)_j^b \rangle \epsilon^{abc} \epsilon_{ijk} \sim Y_k^c. \quad (65)$$

In order to study kaon condensation we have to allow the left and right handed order parameters to be independent. This problem was studied in two papers by Buballa and Forbes<sup>49,50</sup>.

Color and electric charge neutrality are enforced by adding chemical potentials  $(\mu_3, \mu_8, \mu_e)$  for color isospin, color hypercharge and electric charge. In most microscopic calculations the effect of the strange quark mass is taken into account by considering an effective chemical potential  $\mu_s = m_s^2/(2p_F)$  for the strange quark. In Table 1 we list the chemical potentials for the different quark states. The quarks are labeled by color ( $rgb$ ) and flavor ( $uds$ ). They are grouped into the main pairing channels in the CFL phase. We also show the leading order result in the charge neutral CFL phase. In this case we find  $\mu_e = \mu_3 = 0$  and  $\mu_8 = -\mu_s$  and the dominant pair breaking stress occurs in the  $(rs) - (bu)$  and  $(gs) - (bd)$  sector.

We can associate the quark states in the microscopic theory with the baryon fields in the effective theory by computing their quantum numbers under the unbroken  $SU(3)_F$  symmetry. The effective theory is formulated in terms of gauge invariant fields and does not require color chemical potentials. In weak coupling we can derive the effective theory by integrating out gluonic degrees of freedom. In this case the equations of motion for the color gauge potential automatically enforce color neutrality.

We observe that the leading order results in the NJL calculation agree with the results derived from the effective field theory. The comparison was extended to the kaon condensed phase by Forbes<sup>50</sup>. He finds that the  $bu$  (proton) and  $bd$  (neutron) states split, and that the pair breaking stress on both states is reduced. The critical  $\mu_s$  for gapless states is  $\mu_s = 1.2\Delta$ , in qualitative agreement with the leading order EFT result  $\mu_s = 4\Delta/3$ .

Microscopic calculations show that in the CFL phase the gap parameters  $\Delta_{1,2,3}$  are very similar even if the pair breaking stress  $\mu_s$  is close to the value of the gap<sup>37</sup>. The main effect is a reduction of the average gap which is presumably related to the decrease in the common Fermi momentum that occurs if  $\mu_s$  is increased at constant  $\mu_B$ . In the gapless CFL phase, on the other hand, the splitting between the different gap parameters becomes significant. Neither one of these two effects is included in the EFT calculations discussed in Sects. 3.3-3.6. The response of the gap to the trace part of  $MM^\dagger/p_F^2$  can be taken into account by adding a higher order operator to the effective lagrangian equ. (41), but the coefficient of this term is model dependent. Indeed, in perturbative QCD the gap will likely increase if  $p_F$  is lowered. The splitting between the gaps in the gapless CFL is due to the fact that

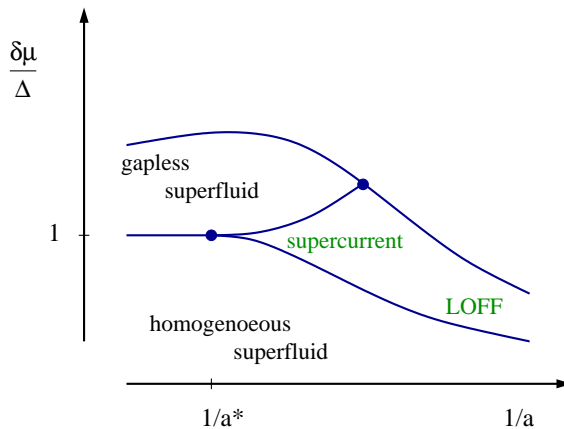


Fig. 10. Conjectured phase diagram for a polarized cold atomic Fermi gas as a function of the scattering length  $a$  and the difference in the chemical potentials  $\delta\mu = \mu_{\uparrow} - \mu_{\downarrow}$ , from Son & Stephanov (2005).

gapless regions on the Fermi surface no longer contribute to pairing. In the EFT treatment this effect is not included because the current is assumed to be much smaller than the gap. Clearly, in the regime where the number of gapless states is large the back-reaction on the gap has to be taken into account.

#### 4. Cold atomic systems

A nice system in which stressed pairing can be studied in the laboratory is a cold dilute gas of fermionic atoms. Using Feshbach resonances it is possible to tune the interaction between the Bose-Einstein (BEC) limit of tightly bound diatomic molecules and the Bardeen-Cooper-Schrieffer (BCS) limit of weakly correlated Cooper pairs. The most interesting part of the phase diagram is the crossover regime where the two-body scattering length diverges.

A conjectured (and, most likely, oversimplified) phase diagram for a polarized gas is shown in Fig. 10. In the BEC limit the gas consists of tightly bound spin singlet molecules. Adding an extra up or down spin requires energy  $\Delta$ . For  $|\delta\mu| = |\mu_{\uparrow} - \mu_{\downarrow}| > \Delta$  the system is a homogeneous mixture of a Bose condensate and a fully polarized Fermi gas. One can show that in the dilute limit this mixture is stable with regard to phase separation<sup>51</sup>.

The Bose-Fermi-gas mixture is a gapless superfluid. We can ask, along the lines of Sect. 3.6, whether the system is stable with respect to the formation of a non-zero supercurrent. We can study this question using the effective lagrangian

$$\mathcal{L} = \psi^{\dagger} \left( i\partial_0 - \epsilon(-i\vec{\partial}) - i(\vec{\partial}\varphi) \cdot \frac{\vec{\partial}}{2m} \right) \psi + \frac{f_t^2}{2} \dot{\varphi}^2 - \frac{f^2}{2} (\vec{\partial}\varphi)^2. \quad (66)$$

Here,  $\psi$  describes a gapless fermion with dispersion law  $\epsilon(\vec{p})$  and  $\varphi$  is the superfluid Goldstone mode. The low energy parameters  $f_t$  and  $f$  are related to the density and

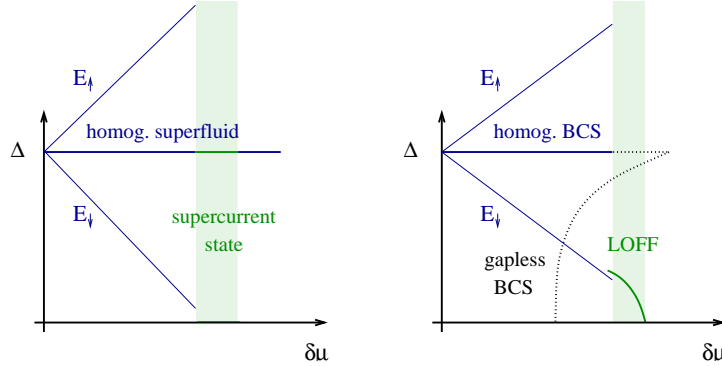


Fig. 11. Schematic behavior of the gap parameter and the quasi-particle energies near the onset of the supercurrent state (left panel) and in the BCS limit (right panel).

the velocity of sound. Similar to the chiral theory discussed in Sect. 3.6 the p-wave coupling of the fermions to the Goldstone boson is governed by the  $U(1)$  symmetry of the theory.

Setting up a current  $\vec{v}_s = \vec{\partial}\varphi/m$  requires energy  $f^2 m^2 v_s^2/2$ . The contribution from fermions can be computed using the fermion dispersion law in the presence of a non-zero current

$$\epsilon_v(\vec{p}) = \epsilon(\vec{p}) + \vec{v}_s \cdot \vec{p} - \delta\mu. \quad (67)$$

The total free energy is

$$F(v_s) = \frac{1}{2} n m v_s^2 + \int \frac{d^3 p}{(2\pi)^3} \epsilon_v(\vec{p}) \Theta(-\epsilon_v(\vec{p})), \quad (68)$$

where  $n$  is the density and we have used  $f^2 = n/m$ . Son and Stephanov noticed that the stability of the gapless phase depends crucially on the nature of the dispersion law  $\epsilon(p)$ . For small momenta we can write  $\epsilon(p) \simeq \epsilon_0 + \alpha p^2 + \beta p^4$ . In the BEC limit  $\alpha > 0$  and the minimum of the dispersion curve is at  $p = 0$  while in the BCS limit  $\alpha < 0$  and the minimum is at  $p \neq 0$ . In the latter case the density of states on the Fermi surface is finite and the system is unstable with respect to the formation of a non-zero current. The free energy functional is of exactly the same type as the one given in equ. (53). On the other hand, if the minimum of the dispersion curve is at zero, then the density of states vanishes and there is no instability. As a consequence there is a critical point along the BEC-BCS line at which the instability will set in.

We can also analyze the system in the BCS limit. This analysis goes back to the work of Larkin, Ovchinnikov, Fulde and Ferrell<sup>52,53</sup>, see the review<sup>54</sup>. First consider homogeneous solutions to the BCS gap equation for  $\delta\mu \neq 0$ . In the regime  $\delta\mu < \Delta_0$  where  $\Delta_0 = \Delta(\delta\mu=0)$  the gap equation has a solution with gap parameter  $\Delta = \Delta_0$ . The free energy of this solution is

$$F = -\frac{N}{4} (\Delta^2 - 2\delta\mu^2), \quad (69)$$

where  $N$  is the density of states on the Fermi surface. For  $\delta\mu > \Delta_0/2$  there is a second solution with  $\Delta = (2\delta\mu\Delta_0 - \Delta_0^2)^{1/2}$ , but this solution is a local maximum of the free energy. There are no gapless modes in the stable BCS phase, but the unstable BCS phase is gapless, see Fig. 11.

For  $\Delta_0 > \delta\mu > \Delta_0/\sqrt{2}$  the gap equation has a non-trivial solution, but the free energy is higher than the free energy of the normal phase and the solution is only meta-stable. LOFF studied whether it is possible to find a stable solution in which the gap has a spatially varying phase

$$\Delta(\vec{x}) = \Delta e^{2i\vec{q}\cdot\vec{x}}. \quad (70)$$

This solution exists in the LOFF window  $\delta\mu_1 < \delta\mu < \delta\mu_2$  with  $\delta\mu_1 = \Delta_0/\sqrt{2} \simeq 0.71\Delta_0$  and  $\delta\mu_2 \simeq 0.754\Delta_0$ . The LOFF momentum  $q$  depends on  $\delta\mu$ . Near  $\delta\mu_2$  we have  $qv_F \simeq 1.2\delta\mu$ . The gap  $\Delta$  goes to zero near  $\delta\mu_2$  and reaches  $\Delta \simeq 0.25\Delta_0$  at  $\delta\mu_1$ .

Clearly, the LOFF solution is of the same type as the supercurrent state. The  $U(1)$  of baryon number is spontaneously broken and the phase of the condensate has a non-zero gradient. The difference is that in the supercurrent state the current is much smaller than the gap,  $v_F(\nabla\varphi) \ll \Delta$ , while in the LOFF phase  $v_F(\nabla\varphi) > \Delta$  (and  $v_F(\nabla\varphi) \gg \Delta$  near  $\delta\mu_2$ ). In the supercurrent state the Fermi surface is mostly gapped but a small shell near one of the pole caps is ungapped. In the weakly coupled LOFF state there are gapless excitations over most of the Fermi surface but pairing takes place near two rings on the northern and southern hemisphere.

In the LOFF state it is energetically favorable to take linear superpositions of equ. (70) with more than one plane wave. As a consequence, the LOFF state has a crystalline structure and there are planes on which the order parameter has a node. In the supercurrent state the current is much smaller than the gap and the formation of nodes is not favored. This implies that there will be at least one phase transition (not shown in Fig. 10) that separates the supercurrent state from the LOFF phase.

## 5. Outlook

Does QCD with three flavors more closely resemble the supercurrent state or the LOFF state of the cold atomic system? In the CFL phase gapless excitations first appear in a regime where the paired state is stable with respect to the normal phase or other homogeneous phases. The resulting instability can be resolved by the formation of a Goldstone boson current  $j < \Delta$ . Whether or not the current is not only numerically but also parametrically small compared to the gap depends on certain details that need to be studied more carefully. In the kaon condensed phase the lowest mode is charged and the current is suppressed by charge neutrality. If the neutral mode becomes gapless, too, or if kaons are not condensed the current is no longer suppressed. Once the current becomes comparable to the gap it may be more appropriate to characterize the system as a LOFF state<sup>56</sup>. In particular,

it is possible that nodes in the condensate appear and quark matter turns into a crystal<sup>55</sup>.

Ultimately we would like to obtain observational evidence for exotic phases of dense matter. Polarized atomic Fermi gases have been created in the laboratory but so far neither the supercurrent state nor the LOFF state have been observed. In the case of quark matter we need to identify unique signatures of the possible phases that can be compared to observational evidence. Much work in this direction remains to be done.

Acknowledgments: The work presented in this review was performed in collaboration with P. Bedaque, D. Kaplan, A. Kryjevski, and K. Schwenzer. I would like to thank M. Alford and A. Sedrakian for Organizing the workshop on “Pairing in fermionic systems: Beyond the BCS theory” at the INT (Seattle). This work is supported in part by the US Department of Energy grant DE-FG-88ER40388.

## References

1. M. Alford, K. Rajagopal and F. Wilczek, Nucl. Phys. **B537**, 443 (1999) [hep-ph/9804403].
2. T. Schäfer, Nucl. Phys. B **575**, 269 (2000) [hep-ph/9909574].
3. N. Evans, J. Hormuzdiar, S. D. Hsu and M. Schwetz, Nucl. Phys. B **581**, 391 (2000) [hep-ph/9910313].
4. M. Alford, J. Berges and K. Rajagopal, Nucl. Phys. **B558**, 219 (1999) [hep-ph/9903502].
5. T. Schäfer and F. Wilczek, Phys. Rev. **D60**, 074014 (1999) [hep-ph/9903503].
6. M. Alford and K. Rajagopal, JHEP **0206**, 031 (2002) [hep-ph/0204001].
7. F. Neumann, M. Buballa and M. Oertel, Nucl. Phys. A **714**, 481 (2003) [hep-ph/0210078].
8. A. W. Steiner, S. Reddy and M. Prakash, Phys. Rev. D **66**, 094007 (2002) [hep-ph/0205201].
9. D. K. Hong, Phys. Lett. B **473**, 118 (2000) [hep-ph/981251].
10. D. K. Hong, Nucl. Phys. B **582**, 451 (2000) [hep-ph/9905523].
11. S. R. Beane, P. F. Bedaque and M. J. Savage, Phys. Lett. B **483**, 131 (2000) [hep-ph/0002209].
12. T. Schäfer and K. Schwenzer, Phys. Rev. D **70**, 054007 (2004) [hep-ph/0405053].
13. E. Braaten and R. D. Pisarski, Phys. Rev. D **45**, 1827 (1992).
14. T. Schäfer and K. Schwenzer, preprint, hep-ph/0512309.
15. B. Vanderheyden and J. Y. Ollitrault, Phys. Rev. D **56**, 5108 (1997).
16. C. Manuel, Phys. Rev. D **62**, 076009 (2000).
17. W. E. Brown, J. T. Liu and H. Ren, Phys. Rev. D **62**, 054013 (2000).
18. A. Ipp, A. Gerhold and A. Rebhan, Phys. Rev. D **69**, 011901 (2004).
19. D. T. Son, Phys. Rev. **D59**, 094019 (1999) [hep-ph/9812287].
20. T. Schäfer and F. Wilczek, Phys. Rev. **D60**, 114033 (1999) [hep-ph/9906512].
21. R. D. Pisarski and D. H. Rischke, Phys. Rev. **D61**, 074017 (2000) [nucl-th/9910056].
22. D. K. Hong, V. A. Miransky, I. A. Shovkovy and L. C. Wijewardhana, Phys. Rev. **D61**, 056001 (2000) [hep-ph/9906478].
23. W. E. Brown, J. T. Liu and H. c. Ren, Phys. Rev. D **61**, 114012 (2000) [hep-ph/9908248].
24. Q. Wang and D. H. Rischke, Phys. Rev. D **65**, 054005 (2002) [nucl-th/0110016].

25. T. Schäfer, Nucl. Phys. A **728**, 251 (2003) [hep-ph/0307074].
26. T. Schäfer, Phys. Rev. D **65**, 074006 (2002) [hep-ph/0109052].
27. G. Baym and S. A. Chin, Nucl. Phys. A **262**, 527 (1976).
28. B. A. Freedman and L. D. McLerran, Phys. Rev. D **16**, 1169 (1977).
29. V. Baluni, Phys. Rev. D **17**, 2092 (1978).
30. E. S. Fraga and P. Romatschke, Phys. Rev. D **71**, 105014 (2005) [hep-ph/0412298].
31. R. Casalbuoni and D. Gatto, Phys. Lett. **B464**, 111 (1999) [hep-ph/9908227].
32. D. T. Son and M. Stephanov, Phys. Rev. **D61**, 074012 (2000) [hep-ph/9910491],  
erratum: hep-ph/0004095.
33. P. F. Bedaque and T. Schäfer, Nucl. Phys. **A697**, 802 (2002) [hep-ph/0105150].
34. T. Schäfer, D. T. Son, M. A. Stephanov, D. Toublan and J. J. M. Verbaarschot,  
Phys. Lett. B **522**, 67 (2001) [hep-ph/0108210].
35. D. B. Kaplan and S. Reddy, Phys. Rev. D **65**, 054042 (2002) [hep-ph/0107265].
36. A. Kryjevski, D. B. Kaplan and T. Schäfer, Phys. Rev. D **71**, 034004 (2005)  
[hep-ph/0404290].
37. M. Alford, C. Kouvaris and K. Rajagopal, Phys. Rev. Lett. **92**, 222001 (2004)  
[hep-ph/0311286].
38. A. Kryjevski and T. Schäfer, Phys. Lett. B **606**, 52 (2005) [hep-ph/0407329].
39. A. Kryjevski and D. Yamada, Phys. Rev. D **71**, 014011 (2005) [hep-ph/0407350].
40. T. Schäfer and F. Wilczek, Phys. Rev. Lett. **82**, 3956 (1999) [hep-ph/9811473].
41. M. Huang and I. A. Shovkovy, Phys. Rev. D **70**, 051501 (2004) [hep-ph/0407049].
42. R. Casalbuoni, R. Gatto, M. Mannarelli, G. Nardulli and M. Ruggieri, Phys. Lett.  
B **605**, 362 (2005) [hep-ph/0410401].
43. T. Schäfer, Phys. Rev. Lett. **96**, 012305 (2006) [hep-ph/0508190].
44. A. Kryjevski, preprint, hep-ph/0508180.
45. D. T. Son and M. A. Stephanov, preprint, cond-mat/0507586.
46. A. Kryjevski and T. Schäfer, in preparation.
47. T. Schäfer, Phys. Rev. D **65**, 094033 (2002) [hep-ph/0201189].
48. S. B. Ruster, I. A. Shovkovy and D. H. Rischke, Nucl. Phys. A **743**, 127 (2004)  
[hep-ph/0405170].
49. M. Buballa, Phys. Lett. B **609**, 57 (2005) [hep-ph/0410397].
50. M. M. Forbes, Phys. Rev. D **72**, 094032 (2005) [hep-ph/0411001].
51. L. Viverit, C. J. Pethick, H. Smith, Phys. Rev. **A61** 053605 (2000)  
[cond-mat/9911080].
52. A. I. Larkin and Yu. N. Ovchinnikov, Zh. Eksp. Theor. Fiz. **47**, 1136 (1964); engl.  
translation: Sov. Phys. JETP **20**, 762 (1965).
53. P. Fulde and A. Ferrell, Phys. Rev. **145**, A550 (1964).
54. R. Casalbuoni and G. Nardulli, Rev. Mod. Phys. **76**, 263 (2004) [hep-ph/0305069].
55. M. G. Alford, J. A. Bowers and K. Rajagopal, Phys. Rev. D **63**, 074016 (2001)  
[hep-ph/0008208].
56. R. Casalbuoni, R. Gatto, N. Ippolito, G. Nardulli and M. Ruggieri, Phys. Lett. B  
**627**, 89 (2005) [hep-ph/0507247].